CRIL: An Efficient Online Adaptive Indoor Localization System

Sheng Cai, *Student Member, IEEE*, Weixian Liao, *Student Member, IEEE*, Changqing Luo, *Student Member, IEEE*, Ming Li, *Member, IEEE*, Xiaoxia Huang, *Member, IEEE*, and Pan Li, *Member, IEEE*

***Abstract*—Indoor localization or indoor positioning systems find their use in many important applications such as augmented reality, guided tours, tracking and monitoring, and situational awareness and have recently attracted intense research interests. Previous localization systems are usually received signal strength indication (RSSI)-based, inertial navigation system (INS)-based, or an integration of these two. However, few of them can account for dynamic communication environments, where channel states constantly change. To the best of our knowledge, this paper is the first to propose an efficient and adaptive indoor localization system called coupled RSSI and INS localization (CRIL), which can adapt to dynamic communication environments quickly and effectively. Moreover, CRIL can account for the uncertainties in RSSI measurements such as varying covariances and outliers as well. Extensive simulation results demonstrate that our proposed CRIL system is able to track both slow changes and sudden changes of the channel states in dynamic environments. Noticeably, the proposed CRIL can perform accurate localization with estimation errors up to 1 m, while previous schemes' localization errors are up to several meters or even tens of meters. Moreover, we test CRIL in real experiments, and its localization error is up to 3 m in dynamic environments.**

***Index Terms*—Dynamic channel states, inertial navigation system (INS), Kalman filter, online localization, received signal strength indication (RSSI).**

I. Introduction

INDOOR localization or indoor positioning systems have found their use in many important applications, including augmented reality [1]; guided tours [2] (e.g., in museums, shopping malls); tracking and monitoring [3], [4]; and situational awareness [5]. For example, social networks help people find friends at a party based on their location information [1]. To enable effective response in disaster rescue, accurate and reliable location information is indispensable as well. However, since global positioning system (GPS) signals are usually poor in indoor environments, how to design an accurate indoor localization system is a challenging problem.

Due to the widespread adoption of wireless local area networks and mobile devices, Wi-Fi signals easily become an alternative of GPS signals for the indoor localization. Some works have proposed indoor localization techniques based on angle of arrival (AOA) [6], time difference of arrival (TDOA) [7], time of arrival (TOA) [8], etc., of the Wi-Fi signals. These methods require extra hardware to measure such data, which is not practical for common mobile devices like smart phones or tablets. Some other works develop schemes by taking advantage of the received signal strength indicator (RSSI), which can be easily obtained by almost every wireless device. Generally, RSSI-based localization can be classified into two categories: *fingerprinting- or mapping-based schemes* [3], [4], [9], [10], and *channel modeling-based schemes* [11]–[13]. The first kind of schemes rely on building the comprehensive data maps of RSSI, which requires significant efforts and needs recalibration whenever the environment changes. The second kind of schemes attempt to construct an accurate channel model to estimate the distances between a receiver and several known transmitters based on measured RSSI values, then employ estimation algorithms such as the circular positioning and the hyperbolic positioning [13], [14] to find the receiver's location. Although the channel modeling-based schemes do not require as much preparatory work as RSSI data mapping-based schemes, they need an accurate channel model, which is difficult to get due to its dynamic nature in indoor environments. Several calibration methods, such as in [15] and [16], are proposed to estimate the parameters in the channel model. Unfortunately, some of them like [15] are passive offline schemes, while the online schemes like [16] require much extra communication and computation cost.

One way to improve the performance of the channel modeling-based localization systems is to integrate it with an inertial navigation system (INS) [17]. In particular, an INS uses an inertial measurement unit (IMU) to estimate an object's position with a high update rate without any other side information. However, the error of the IMU usually gets accumulated very fast, especially for those cheap IMUs on mobile devices, which renders the stand-alone INS impractical. Previous works

Manuscript received April 14, 2016; revised July 10, 2016; accepted July 23, 2016. Date of publication August 2, 2016; date of current version May 12, 2017. This work was supported in part by the U.S. National Science Foundation under Grant CNS-1602172 and Grant CNS-1566479. The work of M. Li was supported in part by the U.S. National Science Foundation under Grant CNS-1566634. The work of X. Huang was supported in part by the Guangdong Science and Technology Project under Grant 2015A010103009, the Shenzhen Science and Technology project under Grant CXZZ20150401152251212, and the NSFC-Guangdong Joint Program under Grant U1501255 and Grant U1301256. The review of this paper was coordinated by Y. Cheng.

S. Cai is with the Department of Electrical and Computer Engineering, Mississippi State University, Starkville, MS 39762 USA (e-mail: sc1222@msstate.edu).

M. Li is with the Department of Computer Science and Engineering, University of Nevada, Reno, NV 89557 USA (e-mail: mingli@unr.edu).

X. Huang is with Shenzhen Institutes of Advanced Technology, Chinese Academy of Sciences, Shenzhen 518055, China (e-mail: xx.huang@siat.ac.cn).

W. Liao, C. Luo, and P. Li are with the Department of Electrical Engineering and Computer Science, Case Western Reserve University, Cleveland, OH 44106 USA (e-mail: wxl393@case.edu; cxl881@case.edu; lipan@case.edu).

Color versions of one or more of the figures in this paper are available online at http://ieeexplore.ieee.org.

Digital Object Identifier 10.1109/TVT.2016.2597303

[18]–[22] propose to couple these two systems by data fusion technologies, but they cannot account for the dynamic channel models in dynamic communication environments.

In this paper, we propose an efficient coupled RSSI and INS localization system called CRIL, which integrate RSSI-based channel modeling localization system with the INS localization system and can adapt to dynamic communication environments quickly and effectively. Specifically, we employ a Kalman filter to fuse the localization results obtained from the RSSI and INS systems. Moreover, we introduce a recursive process in the update phase of the Kalman filter to update the parameters of the channel model utilizing the fused results. In doing so, our system can well model the dynamic communication channels in realtime without much additional calibration or overhead. In addition, we notice that there are always noise and measurement errors in the localization process. To avoid unstable estimation results, we carefully design a stop mechanism to terminate the recursive process. Our recursive method of estimating parameters can be applied to other filters or data fusion technologies to model the changing of a subsystem's parameters. Furthermore, we have developed schemes to reduce outliers in and update the covariance of RSSI measurements.

Our main contributions in this paper are as follows.

1) The proposed CRIL system can proactively track both gradual and abrupt changes in the channel model in realtime, and hence account for dynamic communication environments.
2) CRIL can effectively account for uncertainties in the RSSI measurements through outlier reduction and RSSI covariance update.
3) CRIL can achieve very small localization errors, i.e., much less than 1 m in simulations and up to 3 m in experiments even in dynamic communication environments, compared to large errors (up to tens of meters) by previous localization schemes.

The rest of the paper is organized as follows. Section II reviews previous work on localization systems. In Section III, we present the system models. Section IV describes our proposed CRIL system, which is evaluated in Section V through extensive simulations, and in Section VI through real experiments. Finally, we conclude the paper in Section VII.

II. Related Work

The rising interests in the indoor localization problems have drawn intensive attention. We introduce the most related work below.

Evennou and Marx [3] and Woodman and Harle [4] propose RSSI fingerprinting/mapping-based localization schemes. In particular, Evennou and Marx[3] have developed a system where an accelerometer can count the number of walking steps of the user, a gyroscope can tell the orientation of the user, and the RSSI fingerprinting-based scheme provides the location of the user. Woodman and Harle [4] have done similar work, in which an RSSI mapping scheme is developed to find the location of a user. Besides, Wu *et al.* [23] have designed a channel state information (CSI)-based fingerprinting scheme. All such schemes require significant efforts in advance or whenever the communication environment changes.

TABLE I
Summary of Accuracy of Different Previous Localization Systems

Localization Scheme	Error
RSSI fingerprinting/mapping [9]	1.50 m
CSI-based fingerprinting [23]	1.75 m
RSSI channel modeling [13]	3.69 m
A data fusion-based system [22]	2.29 m

Some previous works [13]–[16], [24] have designed localization schemes through channel modeling utilizing the RSSI. The path loss model with log-normal shadowing is commonly adopted. For instance, to build a more accurate model, Bernardos *et al.* [16] and Barsocchi *et al.* [15] have formulated optimization problems to calibrate the channel model, which needs extra communication and time. As mentioned earlier, these schemes cannot account for dynamic communication channels, which is usually the case in indoor environments where both the objects under observation and the surrounding people/things may move around.

Data fusion algorithms have been designed to integrate RSSI systems with INS systems. Coronel *et al.* [18]–[20] have developed loosely coupled estimation algorithms to fuse the two systems, which means that each of the two subsystems outputs an estimated position and the high level system fuses these results. In contrast, in [21] and [22] tightly coupled estimation algorithms have been designed to fuse both systems, i.e., the high level system will fuse the measurements (angular, velocity, RSSI, etc.) directly from the two subsystems to calculate the final position, and the subsystems will not output their own estimated positions. The former estimation algorithms have lower computational complexity, while the latter estimation algorithms have better performance. Our proposed CRIL system takes advantage of both of them and can perform better.

We summarize the accuracy of a few previous localization systems in Table I. Notice that these results depend on highly accurate measurement devices or good calibrations, and are obtained in static communication environments. In contrast, as we will see later, the proposed CRIL system can achieve much smaller localization errors, i.e., much less than 1 m, even in dynamic communication environments by simulations.

In addition, there are some other localization systems such as those in [21], [25], and [26] which utilize both ultrawide band (UWB) systems and INSs. The use of the UWB enables the measurement of the AOA, TDOA, TOA, etc., but currently, UWB radio interfaces are not very common on mobile devices and would be more expensive.

III. System Models

A. System Architecture

As shown in Fig. 1, we consider an indoor environment where we intend to track a moving pedestrian's (or object's) 2-D location on a certain floor of a building.[1] There are a number of Wi-Fi anchors in known positions in this space. The object carries a

[1] In this paper, we use pedestrian and object interchangeably.

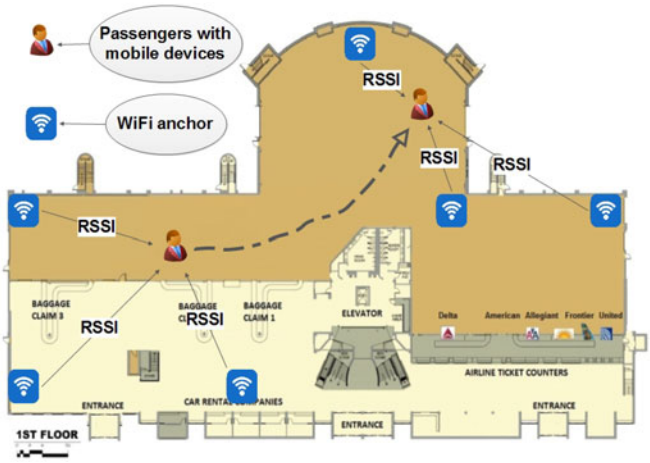

Fig. 1. Typical scenario of indoor localization.

mobile device with a Wi-Fi radio and an IMU. Thus, the object can receive Wi-Fi signals from the anchors and can measure the RSSI of each of the signal. More importantly, we consider a dynamic indoor environment, which implies the dynamic nature of the communication channels therein.

B. Channel Model

One of the most commonly used channel models is the log-normal path loss model [24], which has a direct relationship between the distance and the received signal strength. Specifically, the RSSI (in dBm) of a signal received at a receiver, denoted by P_{RX}, can be calculated as

$$P_{\text{RX}}(dBm) = A - 10\eta \log_{10}(d/d_0) + N_0 \tag{1}$$

where A is the received signal strength at a reference distance d_0, η is the path loss exponent, and N_0 is the noise in the environment. The value of A depends on the transmitted signal power P_{TX} and the antenna gains of the transmitter and the receiver. The noise N_0 is usually defined as a zero-mean Gaussian random variable $\mathcal{N}(0, \sigma)$.

Rewriting (1), the distance d between the transmitter and the receiver can be calculated by

$$d = d_0 \cdot 10^{\frac{A - P_{\text{RX}} + N_0}{10\eta}}. \tag{2}$$

Note that η typically varies between 2 and 4 in outdoor environments, and can range from 4 to 6 in indoor environments [13]. Obviously, time-consuming experiments need to be conducted in order to calibrate the value of η before we use this channel model to estimate the distance d. The overhead becomes more intolerable in dynamic environments where channel models constantly change due to its sensitivity to surrounding movements, temperature, air pressure, air moisture, etc. [27]. Therefore, a real-time calibration process is indispensable to track the changes in the path loss exponent η and, hence, perform more accurate localization.

C. Observation Model

The observation model defines the relation between the measurements and the actual states of the observed object. The proposed CRIL system includes two subsystems: an RSSI localization system and an INS localization system, both of which will output their observation results, i.e., measurement results. Let $\boldsymbol{Z}$ denote the measurement of the observed object's location $\boldsymbol{X} = [x, y]^\top \in \Re_{2\times 1}$. Note that the object's position in the z-axis is denoted by z_* and does not change, which does not need to be estimated. Then, we can have the following observation model:

$$\boldsymbol{Z} = \begin{bmatrix} \boldsymbol{Z}_{\text{INS}} \\ \boldsymbol{Z}_{\text{RSSI}} \end{bmatrix} = \boldsymbol{C}\boldsymbol{X} + \boldsymbol{\Upsilon} \tag{3}$$

where $\boldsymbol{Z}_{\text{INS}}$ and $\boldsymbol{Z}_{\text{RSSI}}$ are the measurements of the object's position from the INS system and RSSI system, respectively, and $\boldsymbol{\Upsilon}$ is the measurement noise. Note that $\boldsymbol{C}$ is the observation matrix which is defined as

$$\boldsymbol{C} = \begin{bmatrix} \boldsymbol{I}_{2\times 2} \\ \boldsymbol{I}_{2\times 2} \end{bmatrix} \tag{4}$$

where $\boldsymbol{I}$ is the identity matrix.

As shown in (3), the observation error affects the measurement results. Thus, the object's position cannot be directly obtained, but need to be estimated based on the measurements.

IV. CRIL: Coupled Received Signal Strength Indicator and Inertial Navigation Localization System

In this section, we detail our proposed online adaptive localization system: CRIL. In particular, the RSSI system has bounded error but a low accuracy, while the INS has a high accuracy in the short run but a large drift error in the long run. Thus, CRIL couples these two systems in order to obtain better localization performance. One salient feature of CRIL is that it can fuse the results from RSSI and INS and, in return, update the channel model in the RSSI in real time. In doing so, CRIL can quickly and efficiently track the dynamic channel model, and better fuse the results from the RSSI and INS to provide more accurate localization results. In what follows, we first describe the RSSI and INS systems and, then, the proposed CRIL localization system.

A. RSSI Localization System

Theoretically, we can determine the location of the object based on the distances between the object and three anchors through triangulation algorithms. However, because of the inaccuracy of the measurement results, the triangulation algorithms cannot be used directly. In the literature, there are mainly two kinds of estimation algorithms that address the inaccuracy problem: the circular positioning algorithm [13], and the hyperbolic positioning algorithm [14]. The circular positioning algorithm minimizes the sum of the squared errors between the real and estimated distances from the tracked object to the different chosen anchors. The hyperbolic positioning algorithm uses a least-squares estimation method to solve a linear problem in order to estimate the object's position. Although the

circular positioning algorithm performs better than the hyperbolic positioning algorithm, it has a much higher computation cost. Considering that the object is usually a mobile device with limited computation capability and energy, we employ the hyperbolic positioning approach.

Specifically, consider that we choose N anchors, and anchor 1 is at the reference spot $(0, 0, 0)$. The square of the distance between the object and an arbitrary anchor i $(1 \leq i \leq N)$, denoted by d_i^2, can be expressed as

$$d_i^2 = (x_i - x)^2 + (y_i - y)^2 + (z_i - z_*)^2. \tag{5}$$

Therefore, subtracting (5) when $i = 1$ from that when $i \neq 1$, we get

$$d_i^2 - d_1^2 = x_i^2 - 2x_i x + y_i^2 - 2y_i y + z_i^2 - 2z_i z_*. \tag{6}$$

Because of the measurement noises and errors, we can only have the estimated distances of d_i, denoted by $\tilde{d}_i$, according to (2). Thus, we rewrite (6) in the following matrix form:

$$\boldsymbol{H}\hat{\boldsymbol{X}} = \tilde{\boldsymbol{b}} \tag{7}$$

where

$$\boldsymbol{H} = \begin{bmatrix} 2x_2 & 2y_2 \\ \vdots & \vdots \\ 2x_N & 2y_N \end{bmatrix}$$

$$\tilde{\boldsymbol{b}} = \begin{bmatrix} x_2^2 + y_2^2 + z_2^2 - 2z_2 z_* - \tilde{d}_2^2 + \tilde{d}_1^2 \\ \vdots \\ x_N^2 + y_N^2 + z_N^2 - 2z_N z_* - \tilde{d}_N^2 + \tilde{d}_1^2 \end{bmatrix}$$

and $\hat{\boldsymbol{X}} = \begin{bmatrix} \hat{x} \\ \hat{y} \end{bmatrix}$ is the estimated position of the object.

The least-squares solution to this equation is

$$\hat{\boldsymbol{X}} = (\boldsymbol{H}^T \boldsymbol{H})^{-1} \boldsymbol{H}^T \tilde{\boldsymbol{b}}. \tag{8}$$

Note that this least-squares solution (8) assigns the same weight to different estimated distances $\tilde{d}_i^2$. However, since the channel model (1) is nonlinear, the same Gaussian distributions of the RSSI measurement error will lead to different distributions of the distance measurement error in the case of different transmission distances. Intuitively, the larger the distance d_i, the larger the distance error caused by the same RSSI error. We employ a weighted hyperbolic algorithm [13] to solve this issue. The algorithm assigns larger weights to those estimated distances with a higher accuracy, under the assumption that the shorter estimated distances have better accuracy as mentioned earlier. The modified weighted least-squares solution is as follows:

$$\hat{\boldsymbol{X}} = (\boldsymbol{H}^T \boldsymbol{S}^{-1} \boldsymbol{H})^{-1} \boldsymbol{H}^T \boldsymbol{S}^{-1} \tilde{\boldsymbol{b}}. \tag{9}$$

Here, $\boldsymbol{S}$ is the estimated covariance matrix of $\tilde{\boldsymbol{b}}$, which can be estimated by

$$\boldsymbol{S} = \begin{bmatrix} \tilde{d}_1^4 + \tilde{d}_2^4 & \tilde{d}_1^4 & \cdots & \tilde{d}_1^4 \\ \tilde{d}_1^4 & \tilde{d}_1^4 + \tilde{d}_3^4 & \cdots & \tilde{d}_1^4 \\ \vdots & \vdots & \ddots & \vdots \\ \tilde{d}_1^4 & \tilde{d}_1^4 & \cdots & \tilde{d}_1^4 + \tilde{d}_N^4 \end{bmatrix}. \tag{10}$$

Note that N should be at least 3 in order for us to conduct the least-squares estimation and have a fairly good estimation of $\boldsymbol{X}$. Due to matrix inversion and matrix multiplication, the computational complexity of finding $\hat{\boldsymbol{X}}$ is $O(N^3)$. The complexity of this algorithm can be very low in practice since N can usually be a small number in real implementations. Moreover, when the RSSI system receives a large number of signals, it can drop those low-quality ones to further reduce the complexity of the computation.

B. Inertial Navigation System

An INS uses an IMU to estimate positions and is widely used as the navigation system for airplane, ships, rockets, etc. [17]. Advances of the micro electro mechanical system (MEMS) technology lead to cheap and small IMUs for common mobile devices like smart phones and tablets. The main advantage of IMUs is that they need no external inputs for measuring their positions and can be used in indoor environments or wherever satellite signals are not available.

Normally, an IMU includes a gyroscope and an accelerometer. In particular, the gyroscope outputs the angular velocity of the object and the accelerometer outputs the linear acceleration. The angular velocity of an object gives its attitude by one integration, which indicates the object's yaw, pitch, and roll. Based on the attitude and other information, we can transfer the linear acceleration in inertial reference coordinates into navigation reference coordinates. Then, based on the Newton's laws of motion, the position of the object can be calculated after two integrations. More detailed descriptions on INS systems can be found in [17].

Therefore, an IMU position estimation system can be modeled by the following linear equations [19]:

$$\bar{\boldsymbol{\phi}}_{j+1} = \bar{\boldsymbol{\phi}}_j + \bar{\boldsymbol{W}}_{j+1}\Delta t + \boldsymbol{\Gamma}_{\boldsymbol{\phi}} \tag{11}$$

$$\bar{\boldsymbol{V}}_{j+1} = \bar{\boldsymbol{V}}_j + \bar{\boldsymbol{A}}_{j+1}\Delta t + \boldsymbol{\Gamma}_{\boldsymbol{V}} \tag{12}$$

$$\bar{\boldsymbol{X}}_{j+1} = \bar{\boldsymbol{X}}_j + \bar{\boldsymbol{V}}_{j+1}\Delta t + \boldsymbol{\Gamma}_{\boldsymbol{X}} \tag{13}$$

where Δt is the IMU's sampling period; and $\bar{\boldsymbol{\phi}}$, $\bar{\boldsymbol{W}}$, $\bar{\boldsymbol{A}}$, $\bar{\boldsymbol{V}}$, and $\bar{\boldsymbol{X}}$ are the attitude vector, angular velocity vector, acceleration vector (calculated based on $\bar{\boldsymbol{\phi}}$ as mentioned earlier), velocity vector, and position vector, respectively, in the navigation reference coordinates. $\boldsymbol{\Gamma}_{\boldsymbol{\phi}}$, $\boldsymbol{\Gamma}_{\boldsymbol{V}}$, and $\boldsymbol{\Gamma}_{\boldsymbol{X}}$ are the noises in $\bar{\boldsymbol{\phi}}$, $\bar{\boldsymbol{V}}$, and $\bar{\boldsymbol{X}}$, respectively, and are assumed to follow Gaussian distribution.

One problem of the INS system is that the accumulated error, which is well known as an INS drift, can increase very fast as time goes by. To be more prominent, as shown in (11)–(13), the error introduced in the angular velocity measurement will be propagated into the estimated attitudes, and the error introduced in the linear acceleration measurement will be propagated into both the estimated velocity and the estimated objects' position. Moreover, since the $(j+1)$th estimated position is based on the previous estimated position $\bar{\boldsymbol{X}}_j$, the previous errors of the INS system will be accumulated into the future position estimations [17]. Therefore, after a few position updates, the accumulated errors may become noneligible. This problem becomes even

more serious in MEMS IMUs because the thermo-mechanical white noise and the bias errors account for a significant fraction of the measurement error [17].

To address the above problem, we propose to employ the pedestrian dead-reckoning (PDR) method [28]–[30], which obtains a pedestrian's position based on the number of steps, step length, and orientation. There are three processes in PDR: step detection, stride length (SL) estimation, and orientation estimation.

1) Step Detection: In this process, the algorithm counts the number of steps by detecting the number of swing phases. Particularly, we first calculate the magnitude of the acceleration a_{j+1} with the three-axis accelerometer [29]

$$a_{j+1} = \sqrt{a_{x_{j+1}}^2 + a_{y_{j+1}}^2 + a_{z_{j+1}}^2} \tag{14}$$

and then identify a swing phase whenever the magnitude a_{j+1} is larger than a threshold T_{acc}.

2) SL Estimation: The zero velocity updates SL algorithm is widely used with a high accuracy for most statuses of a user (walk or run) [29]. In particular, when the user is in the stance phase, the velocity is zero. Using this information, the algorithm can correct the drifts of the accelerometer and decrease the SL errors in the swing phases when we employ (11)–(13).

There are three steps to estimate the length of the ith stride (or the ith swing phase) denoted by SL_i [29]. First, we use (12) to calculate the linear velocities in the duration of swing phase i. Note that a swing phase usually contains a number of IMU's sampling periods. Second, we correct the drifts as follows: The velocities are decreased by the linear interpolation of μ_i, i.e., the mean velocity at the stance phase i, and μ_{i-1} [29]. Third, we carry out the integration of (12) to get the position increment, whose abstract value is the SL SL_i.

3) Orientation Estimation: There are two main methods to estimate the orientation of the pedestrian in the ith stance phase (before the ith swing phase), denoted by θ_{stance_i}, based on the IMU on his/her mobile device: the gyroscope method and the accelerometer method. In the gyroscope method, by using (11), the INS system can output the orientation $\theta_{i,\text{gyro}}$. Although the gyroscope method can give accurate results in a short time period, the drift will increase with time. On the other hand, the accelerometer method is less accurate but does not accumulate the errors as time goes by. Thus, we combine these two methods as follows by introducing a control parameter γ_i $(0 \le \gamma_i \le 1)$

$$\theta_{\text{stance}_i} = (1-\gamma_i)\cdot\theta_{i,\text{acc}} + \gamma_i \cdot \theta_{i,\text{gyro}}. \tag{15}$$

Consequently, when we have all the above results, we can update the user's position after every m steps. Particularly, the $(k+1)$th estimated position, denoted by $\bar{\boldsymbol{X}}_{k+1}$, can be calculated as

$$X_{k+1}^x = X_k^x + \sum_{i=1}^{m} \text{SL}_i \cdot \cos(\theta_{\text{stance}_i}) \tag{16}$$

$$X_{k+1}^y = X_k^y + \sum_{i=1}^{m} \text{SL}_i \cdot \sin(\theta_{\text{stance}_i}). \tag{17}$$

C. Coupling RSSI and INS Systems Through a Kalman Filter

In this section, we develop a new Kalman filter that can well integrate the above RSSI and INS systems to estimate the object's position.

Specifically, Kalman filters are widely used in the data fusion and state estimation [31], and many Kalman filters [32] have been proposed to solve different problems. These different forms of Kalman filters follow the same two general steps: *the prediction (or propagation) step* and *the update step*. In the *prediction step*, the system states are propagated from the last iteration to the predicted states in the current iteration and the prior distribution is generated by using the estimated model of the system. In the *update step*, the filter has two kinds of information: the prior distribution from the *prediction step* and the measurement information. By using the measurement information and the prior distributions of the states, the filter can estimate the posterior distribution of the states and generate the current estimated states.

In what follows, we detail our Kalman filter design. Note that in the following equations, the index k denotes the iteration number, the index $k|k-1$ denotes the predicted parameters, and the $k|k$ denotes the estimated parameters.

First, in the *prediction step*, the filter uses the estimation model (13) to get a predicted state $\boldsymbol{X'}_{k|k-1}$ and the predicted estimated state covariance $\boldsymbol{P}_{k|k-1}$ (or the prior distributions of the states)

$$\boldsymbol{X'}_{k|k-1} = \boldsymbol{X'}_{k-1|k-1} + \bar{\boldsymbol{V}}\Delta T \tag{18}$$

$$\boldsymbol{P}_{k|k-1} = \boldsymbol{P}_{k-1|k-1} + \boldsymbol{Q}_k \tag{19}$$

where ΔT is the update period of the Kalman filter, $\boldsymbol{P}_{k-1|k-1}$ is the covariance matrix of the estimated state vector $\boldsymbol{X'}_{k-1|k-1}$ at time $k-1$, and $\boldsymbol{Q}_k$ is the covariance matrix of the current process noise's distribution. $\boldsymbol{Q}_k$ can be calculated as [22]

$$\boldsymbol{Q}_k = \boldsymbol{I}\cdot\left(\frac{1}{2}\sigma_a\Delta T^2\right)^2 + \boldsymbol{I}\cdot(\sigma_v\Delta T)^2 \tag{20}$$

where $\boldsymbol{I}$ is the identity matrix, and σ_a and σ_v are the standard deviation of the acceleration and of the velocity of the IMU, respectively.

Then, when the system receives enough measurement information from both of the subsystems, the Kalman filter estimates the posterior distribution of the states and generates the current estimated states. Specifically, the *update step* generates the Kalman gain, estimated state, and covariance matrix of the estimated state for the next iteration. Such updates can be made by

$$\boldsymbol{K}_k = \boldsymbol{P}_{k|k-1}\boldsymbol{C}(\boldsymbol{C}\boldsymbol{P}_{k|k-1}\boldsymbol{C}^T + \boldsymbol{R}_k)^{-1} \tag{21}$$

$$\boldsymbol{X'}_{k|k} = \boldsymbol{X'}_{k|k-1} + \boldsymbol{K}_k(\boldsymbol{Z}_k - \boldsymbol{C}\boldsymbol{X'}_{k|k-1}) \tag{22}$$

$$\boldsymbol{P}_{k|k} = (\boldsymbol{I} - \boldsymbol{K}_k\boldsymbol{C})\boldsymbol{P}_{k|k-1} \tag{23}$$

where $\boldsymbol{Z}_k$ is the observation result from the RSSI system and INS system as shown in (9), (16), and (17), respectively, $\boldsymbol{K}_k$ is the optimal Kalman gain, and $\boldsymbol{R}_k$ is the covariance matrix of

the measurement error $\boldsymbol{\Upsilon}_k$

$$\boldsymbol{R}_k = \begin{bmatrix} \boldsymbol{Q}_{k/\text{INS}} & 0 \\ 0 & \boldsymbol{R}_{k/\text{RSSI}} \end{bmatrix}. \tag{24}$$

The entry $\boldsymbol{Q}_{k/\text{INS}}$ corresponding to the INS system is the same as $\boldsymbol{Q}_k$, and $\boldsymbol{R}_{k/\text{RSSI}}$ is the covariance matrix of the RSSI system's results. The initial $\boldsymbol{R}_{0/\text{RSSI}}$ can be given by

$$\boldsymbol{R}_{0/\text{RSSI}} = \boldsymbol{I} \cdot \sigma_R^2 \tag{25}$$

where σ_R is standard deviation of the RSSI system's results that could be predetermined by a few experiments. We will see later that $\boldsymbol{R}_{k/\text{RSSI}}$ will be updated in the algorithm.

Note that as shown in (22), we can fuse the results from the RSSI and INS systems by using the Kalman gain $\boldsymbol{K}_k$ (21).

D. Realtime Update of the Channel Model

As indicated in Section III, the RSSI system's accuracy is directly influenced by the measurement accuracy of the path loss exponent η. However, this value is difficult to obtain in a dynamic environment, where η needs to be obtained experimentally every time we need an estimated position from the RSSI system. Thus, even if η can be accurately calibrated at the beginning of the estimation, η will continue to change because of the dynamic nature of the environment. Some prior works [15], [16] claim that their systems can update the path loss exponent η by using some fixed Wi-Fi anchors and reference points, however, their update is not realtime or accurate enough to catch the changing of the actual parameters.

Different from the previous works, we update the path loss exponent η by recursively using the results of the proposed Kalman filter. The basic idea is to use the Kalman filter's estimation results as the position state input to calibrate the new path loss exponent η. In particular, according to (1), we can easily calculate η as follows:

$$\eta_{\text{new}} = \frac{(A - P_{\text{RX}})}{10 \log \left(\left\| \boldsymbol{X'}_{k|k} - \boldsymbol{X}_{\text{anchor}-i} \right\|_2 / d_0 \right)} \tag{26}$$

where $\boldsymbol{X'}_{k|k}$ and $\boldsymbol{X}_{\text{anchor}-i}$ are the estimated position obtained from the Kalman filter and the position of anchor i, respectively, $\|\|_2$ is the Euclidean norm, and η_{new} is the updated path loss exponent based on the newly obtained estimated position from the Kalman filter. After we have an updated η_{new}, we employ the Kalman filter again to update $\boldsymbol{X'}_{k|k}$, which is then used to update η_{new} again. This process proceeds recursively until we have a good enough estimate of the path loss exponent, which is finally used to update η. Moreover, as will be shown in simulations, the iteration number in the recursive process is very small (mostly no more than 3), which means that this proposed calibration is very efficient.

1) Stop Condition for the Recursive Update Process for η: In the proposed scheme, it is important to find the correct condition to stop the recursive steps for updating η so that we can avoid the influence of the noise and measurement errors. In particular, as shown in the path loss function (1), there is always some noise that affects the accuracy of the RSSI system. Besides, the received signal strength P_{RX} may not be very accurate either. Similarly, there is a noise and measurement error in the INS system as well. The estimated position $\boldsymbol{X'}$ by the coupled Kalman filter thus still contains uncertainty. Since the new pass loss exponent η is calculated according to (26), it is also influenced by these errors. Thus, we decide to set a suitable threshold to avoid getting an unstable η in this recursive process.

Particularly, if the newly estimated position $\boldsymbol{X'}\text{new}_{k|k}$ based on the new path loss exponent η in any iteration is away from the previously estimated position $\boldsymbol{X'}\text{old}_{k|k}$ by a threshold T, it means that the pass loss exponent η did change and the update of η is necessary. Otherwise, the change of the pass loss exponent η may be due to the noise and measurement errors, and the system will ignore this update and terminate the recursive process of updating η. We notice that as shown in (23), the covariance matrix $\boldsymbol{P}_{k|k}$ of the estimated states can be used to obtain a confident range of the estimated position. Therefore, the threshold T can be set to

$$T = \alpha \sqrt{({\sigma_x}^2 + \sigma_y^2)/2} \tag{27}$$

where σ_x^2 and σ_y^2 are the covariances of the estimated position's coordinates x and y in $\boldsymbol{P}_{k|k}$, respectively, and α is a coefficient needed to be tuned. In so doing, our recursive algorithm can generate a threshold online to control the recursive level so that the update of the pass loss exponent η will converge.

2) Online Updating of the RSSI Measurement Error Covariance: Moreover, after the pass loss exponent η is finally updated, as mentioned earlier, some other parameters in the Kalman filter should be updated as well.

Specifically, since the channel model is updated, the measurement covariance $\boldsymbol{R}_k$ needs to be updated accordingly. Rewriting the path loss function (1), we can know that the measurement $\tilde{d}_i$ is a random variable

$$\tilde{d}_i = d_i \cdot 10^{\frac{\mathcal{N}(0,\sigma)}{10\eta}} = 10^{\mathcal{N}(\log_{10} d_i, \frac{\sigma}{10\eta})}. \tag{28}$$

From (28), we find that when the pass loss exponent η is updated, the covariance of the Gaussian distribution changes, and are inversely proportional. Therefore, when the proposed Kalman filter changes the pass loss exponent η, the new variance of the RSSI measurement error is updated as follows:

$$\sigma_{R/\text{new}} = \frac{\eta_{\text{old}}}{\eta_{\text{new}}} \cdot \sigma_{R/\text{old}}. \tag{29}$$

After obtaining these new variances, the Kalman gain $\boldsymbol{K}_k$ and the estimated position $\boldsymbol{X'}_{k|k}$ will also be updated.

E. Further Improvement

1) Online Reduction of RSSI Signal Outliers via L_1 Regression: We notice that RSSI measurements tend to have outliers because of unstable communications or disturbances caused by obstacles [33]. The performance of the Kalman filter will be seriously degraded by the outliers, and therefore, many robust schemes have been proposed to reduce them [34]–[38]. In this paper, we employ an L_1 regression-based approach [34], [38] due to their convenient implementation and low computation complexity.

Specifically, in the proposed Kalman filter, we consider that the RSSI measurement error $\boldsymbol{v}_{k/\text{RSSI}}$ is given by

$$\boldsymbol{v}_{k/\text{RSSI}} = \boldsymbol{r}_{k/\text{RSSI}} + \boldsymbol{o}_{k/\text{RSSI}} \tag{30}$$

where $\boldsymbol{r}_{k/\text{RSSI}}$ and $\boldsymbol{o}_{k/\text{RSSI}}$ are the Gaussian noise and outlier in the step k, respectively.

Then, we can estimate $\boldsymbol{o}_{k/\text{RSSI}}$ by solving the following optimization problem [38]:

$$\min_{\boldsymbol{o}_{k/\text{RSSI}}} (\boldsymbol{v}_{k/\text{RSSI}} - \boldsymbol{o}_{k/\text{RSSI}})^T \boldsymbol{W}_k (\boldsymbol{v}_{k/\text{RSSI}} - \boldsymbol{o}_{k/\text{RSSI}}) + \lambda \left\| \boldsymbol{o}_{k/\text{RSSI}} \right\|_1 \tag{31}$$

where

$$\boldsymbol{W}_k = (\boldsymbol{I} - \boldsymbol{K}_k)^T \boldsymbol{R}_{k/\text{RSSI}}^{-1} (\boldsymbol{I} - \boldsymbol{K}_k) + \boldsymbol{K}_k^T \boldsymbol{P}_{k|k-1}^{-1} \boldsymbol{K}_k.$$

$\|\cdot\|_1$ is a L_1 norm, and λ is a regularization parameter which is needed to get the solution.

The solution to (31) can be obtained by [39]

$$\boldsymbol{o}_{k/\text{RSSI}} = \begin{cases} \boldsymbol{v}_{k/\text{RSSI}} - \frac{\lambda}{2\boldsymbol{W}}, \text{ if } \boldsymbol{v}_{k/\text{RSSI}} > \frac{\lambda}{2\boldsymbol{W}} \\ 0, \text{ if } -\frac{\lambda}{2\boldsymbol{W}} \le \boldsymbol{v}_{k/\text{RSSI}} \le \frac{\lambda}{2\boldsymbol{W}} \\ \boldsymbol{v}_{k/\text{RSSI}} + \frac{\lambda}{2\boldsymbol{W}}, \text{ if } \boldsymbol{v}_{k/\text{RSSI}} < -\frac{\lambda}{2\boldsymbol{W}} \end{cases} \tag{32}$$

where $\boldsymbol{v}_{k/\text{RSSI}} = \boldsymbol{Z}_{k|\text{RSSI}} - \boldsymbol{X'}_{k|k-1}$, and $\frac{\lambda}{2\boldsymbol{W}}$ is used as a threshold to cut the outlier. We set $\frac{\lambda}{2\boldsymbol{W}}$ to the standard deviation of $\boldsymbol{v}_{k/\text{RSSI}}$ which is defined by

$$\boldsymbol{\Sigma}^2_{\boldsymbol{v}_{k/\text{RSSI}}} = \boldsymbol{P}_{k|k-1} + \boldsymbol{R}_{k/\text{RSSI}}. \tag{33}$$

Therefore, λ can be set to

$$\boldsymbol{\lambda} = 2\boldsymbol{W_k}\boldsymbol{\Sigma}_{\boldsymbol{v}_{k/\text{RSSI}}}. \tag{34}$$

By calculating the outliers, we can reduce them from the RSSI measurements $\boldsymbol{Z}_{k/\text{RSSI}}$.

2) Online Estimation for the RSSI Measurement Covariance: As mentioned earlier, the RSSI measurements have outliers which can now be removed. This enables us to have a more accurate estimate of the RSSI measurement error covariance $\boldsymbol{R}_{k/\text{RSSI}}$. Besides, the change in the environment may lead to different $\boldsymbol{R}_{k/\text{RSSI}}$'s. Therefore, before we update $\boldsymbol{R}_{k/\text{RSSI}}$ using (29) when we conduct realtime update of the channel model as described in Section IV-D, we need to obtain $\boldsymbol{R}_{k/\text{RSSI}}$ by using the RSSI measurements without outliers.

In particular, let $\boldsymbol{v}'_{j/\text{RSSI}}$ be equal to $\boldsymbol{v}_{j/\text{RSSI}}$ minus the outlier. Based on the adaptive Kalman filter from [40], the covariance of $\boldsymbol{v}'_{k/\text{RSSI}}$ can be estimated by

$$\boldsymbol{C}_{\boldsymbol{v}'_{k/\text{RSSI}}} = \frac{1}{N} \sum_{j=k-N+1}^{k} \boldsymbol{v}'_{j/\text{RSSI}} {\boldsymbol{v}'_{j/\text{RSSI}}}^T \tag{35}$$

where N is the estimation window size. Then, from (33), the RSSI measurement error covariance can be calculated as

$$\hat{\boldsymbol{R}}_{k/\text{RSSI}} = \boldsymbol{C}_{\hat{\boldsymbol{v}}_{k/\text{RSSI}}} - \boldsymbol{P}_{k|k-1} \tag{36}$$

and then, we can update $\boldsymbol{R}_{k/\text{RSSI}}$ as follows:

Algorithm 1: A Coupled RSSI and INS Localization System.

procedure CRIL($\boldsymbol{X'}_{0|0}$, $\boldsymbol{P}_{0|0}$, $\boldsymbol{Q}_1$, $\boldsymbol{R}_1$)
  Collect the position result from the INS system by (16) and (17).
  Collect the position result from the RSSI system by (9).
  Deduce the RSSI outlier $\boldsymbol{o}_{k/\text{RSSI}}$ and estimate the RSSI measurement covariance $\boldsymbol{R}_{k/\text{RSSI}}$ by (32) and (37), respectively.
  Denote their own position results as $\boldsymbol{Z}_k^{\text{old}}$.
  Compute (18), (19) to estimate predicted states $\boldsymbol{X'}_{k|k-1}$ and predicted covariance $\boldsymbol{P}_{k|k-1}$.
  Calculate Kalman gain K_k by (21) and estimate the estimated position $\boldsymbol{X'}\text{old}_{k|k}$ by (22) by using the measurement $\boldsymbol{Z}_k^{\text{old}}$.
  Use the estimated position $\boldsymbol{X'}\text{old}_{k|k}$ to get the new path loss exponent η^{new} by (26), and the new RSSI position result $\boldsymbol{Z}_{k/\text{RSSI}}$.
  Calculate the new estimated position $\boldsymbol{X'}\text{new}_{k|k}$ with the new RSSI results and new η^{new} by (22).
  while $\left\| \boldsymbol{X'}^{\text{new}}_{k|k} - \boldsymbol{X'}^{\text{old}}_{k|k} \right\|_2 > T$ **do**
    Set $\boldsymbol{X'}\text{old}_{k|k} \leftarrow \boldsymbol{X'}\text{new}_{k|k}$
    Update the path loss exponent η, and RSSI position result $\boldsymbol{Z}_{k/\text{RSSI}}$.
    Calculate the new estimated position $\boldsymbol{X'}\text{new}_{k|k}$ by (22).
  end while
  Update the RSSI measurement covariance $\sigma_{R/\text{new}}$ by (29).
  Update Kalman gain K_k and $\boldsymbol{P}_{k|k}$, and calculate final estimated position $\boldsymbol{X'}^{\text{Final}}_{k|k}$.
end procedure

$$\boldsymbol{R}_{k/\text{RSSI}} = (1-\beta)\boldsymbol{R}_{k-1/\text{RSSI}} + \beta\hat{\boldsymbol{R}}_{k/\text{RSSI}} \tag{37}$$

where β is a control parameter.

The complete algorithm description for CRIL is detailed in Algorithm 1.

V. Simulation Results

In this section, we analyze the performance of our proposed CRIL system through extensive simulations and validate the proposed scheme by comparing it with the following two previous methods:

1) RSSI localization system (RSSI) [13]: With a fixed time step, the RSSI localization system estimates the object's position based on the RSSI values only.
2) A hybrid RSSI and INS system with Kalman filter without channel model update (KF) [20]: Kalman filter is employed to fuse the results from the RSSI system and

the INS system, but there is no channel model update process.

As will be seen later, our proposed system gives very accurate and stable localization results, even in dynamic environments.

A. Simulation Environment and Parameter Setting

In the simulations, we consider that there are three Wi-Fi anchors located at three fixed points, respectively, in a room of 50 m $\times$ 50 m. The tracked object moves around under the coverage of all three anchors, and they are all on the same plane. These anchors send Wi-Fi signals to the tracked object at a fixed rate of one per 0.5 s. The speed of the object is fixed at 1 m/s.

At the start point (5, 5, 5), the object uses its exact position to initialize the parameters and position states in the proposed Kalman filter. The values of σ_a and σ_v in the covariance matrix $\boldsymbol{Q}_k$ of the process noise $\boldsymbol{\Gamma}_{\mathbf{X}}$ are set to 0.1 m/s^2 and 0.1 m/s. In the covariance matrix of the RSSI measurement noise, i.e., $\boldsymbol{R}_{\text{RSSI}}$, the initial value of σ_R is set to 2 m. As explained in the previous section, this $\boldsymbol{R}_{k/\text{RSSI}}$ will be updated online to enhance the accuracy of our algorithm.

The simulations are conducted in MATLAB, where the related models (i.e., RSSI and INS systems) are developed accordingly. The log-normal shadowing path loss model is used as the signal propagation model, where $\sigma = 2$ dBm, and $A = -38.0460$ dBm.

B. Results Under Constant Path Loss Exponent

In this simulation, the real path loss exponent is set to a constant value of 4. As shown in the description of the CRIL algorithm, the noise influences the accuracy of the estimated path loss exponent η. In this special situation where the real path loss exponent η is not changing, the proposed recursive update process for η should keep the estimated η unchanged. The small variation of the estimated η caused by the noise should be ignored by the recursive update process. That means the new CRIL system should have the same performance as the KF method [20].

Specifically, we can see in Fig. 2 that the estimated path loss exponent η (i.e., blue circles in Fig. 2) is unchanged. This is because the proposed recursive update process for η ignores the influence of noise, and the updated η_{new} obtained in the recursive update process (i.e., blue squares in Fig. 2, only one iteration) is not accepted by the system. The results in Fig. 2 validate the design of the proposed threshold T for controlling the recursive level of the update process and shows that we can have a stable and converging update process in this environment with a constant path loss exponent.

In Figs. 3 and 4, we show the estimated positions by our proposed CRIL and by RSSI [13] and KF [20], respectively. We can see that both our CRIL and KF [20] can track the objects' real positions well, with localization errors on the scale of centimeters. The localization errors of RSSI [13] are larger, up to 2.5 m. Figs. 2 and 3 together demonstrate that the proposed recursive update process for η can perform well, even when the noise and the measurement errors influence the estimation of η.

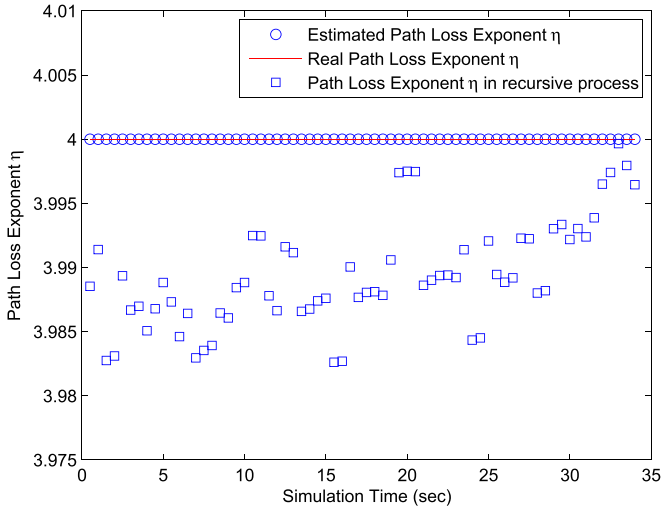

Fig. 2. Estimated path loss exponent η by CRIL.

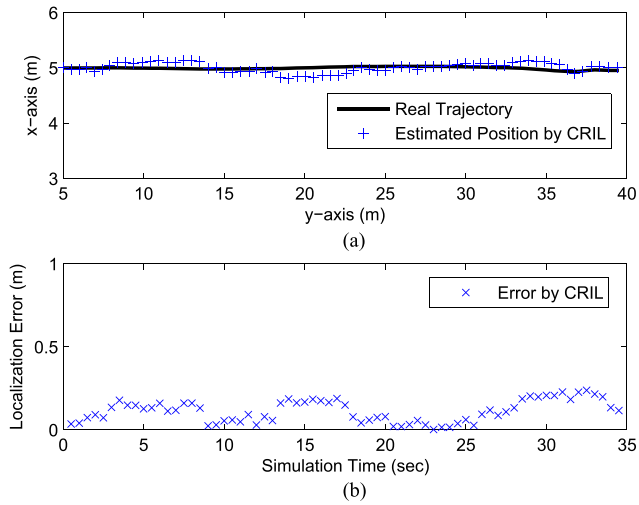

Fig. 3. Comparison of estimated positions by CRIL and the real trajectory. (a) Estimated Positions and Real Trajectory (b) Localization Error.

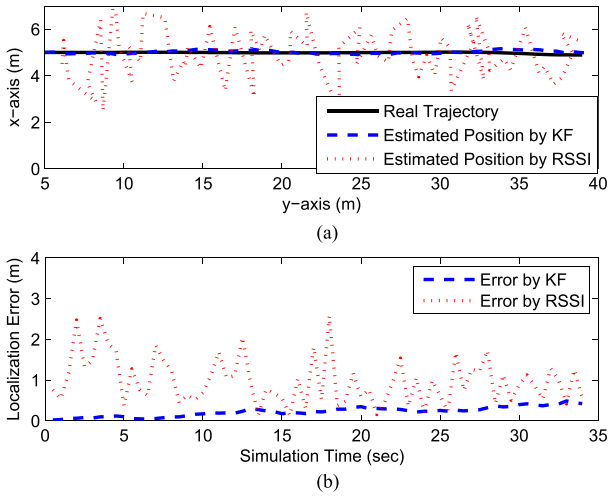

Fig. 4. Comparison of estimated positions by RSSI [13], KF [20], and the real trajectory. (a) Estimated positions and real trajectory. (b) Localization error.

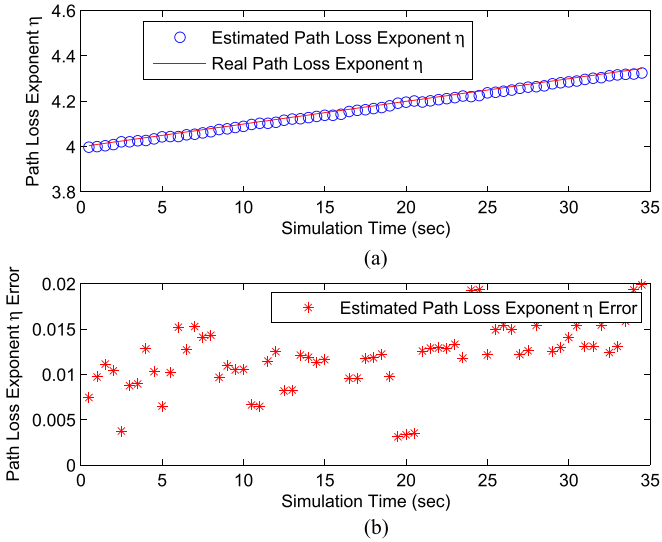

Fig. 5. Comparison of estimated path loss exponent η by CRIL and the real path loss exponent, η which is slowly changing. (a) Path loss exponent h. (b) Estimated path loss exponent h error.

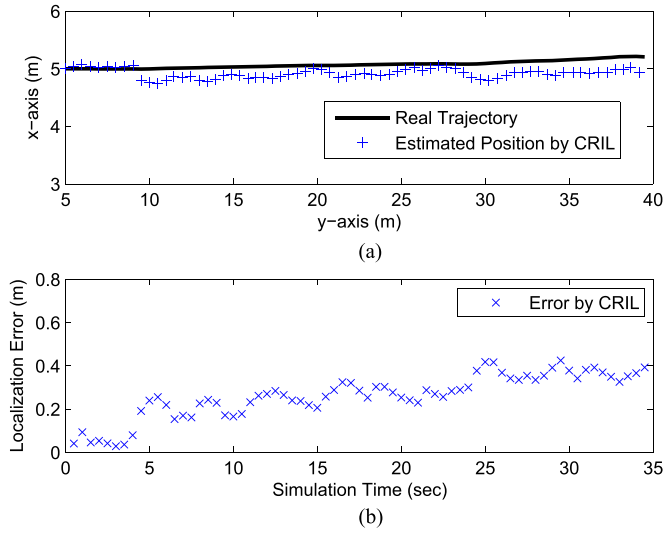

Fig. 6. Comparison of estimated positions by CRIL and the real trajectory with the slowly changing path loss exponent η. (a) Estimated positions and real trajectory. (b) Localization error.

C. Results Under Dynamic Path Loss Exponent

Previous results show that the proposed CRIL system can obtain the same accuracy level as the normal Kalman filter when the path loss exponent is a constant. On the other hand, one of CRIL's biggest advantages is that it can estimate and update the path loss exponent η through a realtime calibration. This is one main reason that the proposed system can have a high localization accuracy compared to the previous RSSI-alone localization systems and hybrid localization systems.

In what follows, two situations are discussed and investigated: first, the value of the real path loss exponent η slowly changes with time; second, the value of the real path loss exponent η has a sudden change, i.e., jumps from one value to another. In the next two sections, we show that the proposed CRIL can achieve an accurate localization in both situations.

1) Path Loss Exponent η is Slowly Changing: In this simulation, the real path loss exponent η slowly changes from 4 to 4.35. This can happen when the humidity in the room is slowly increasing [27]. In Fig. 5, the estimation error of the path loss exponent is very small, and most of the errors are below 0.02. The estimated path loss exponent η can follow the slow changing of the real path loss exponent η. Although there are still some small errors caused by the noise and measurement errors, the estimated path loss exponent η is very accurate and can give very good performance.

Figs. 6 and 7 demonstrate the localization performance of CRIL and of RSSI [13] and KF [20], respectively. Specifically, in Fig. 6, the proposed CRIL system achieves similar performance under dynamic path loss exponents to that in Fig. 3, where the path loss exponent is a constant. The variation of the real path loss exponent η does not influence the accuracy of the proposed CRIL system much. This is because the recursive update process for η can detect this variation efficiently and accurately. We also notice that our proposed scheme's performance (with localization errors up to 0.4 m) is much better than the RSSI [13] and KF [20] localization systems, as shown in Fig. 7. The KF scheme leads to localization errors of a few meters, which cannot be used. The RSSI method is even worse than the KF scheme and has localization errors more than 20 m, due to the inaccurate channel model. From these results, we can see that the proposed CRIL system can fully utilize the fused results of the INS and RSSI systems and detect the variations of the path loss exponent η quickly, thus improving the localization performance. Moreover, as shown in Fig. 8, we notice that the number of iteration numbers in the recursive update process for η are no more than 3, which demonstrates that the proposed update process is very efficient.

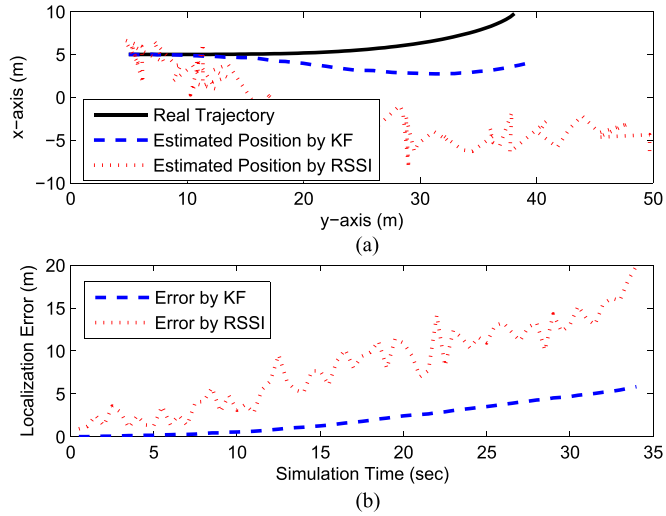

Fig. 7. Comparison of estimated positions by KF [20] and RSSI [13] and the real trajectory with the slowly changing path loss exponent η. (a) Estimated positions and real trajecotry. (b) Localization error.

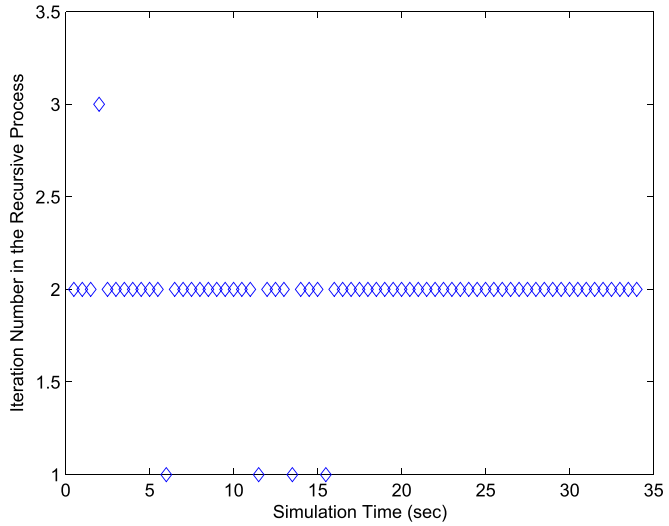

Fig. 8. Number of iterations in the recursive update process for η when η is slowly changing.

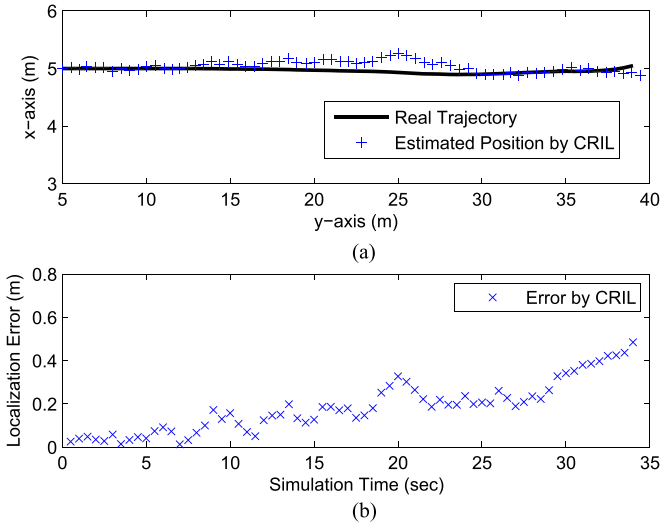

Fig. 10. Comparison of estimated positions by CRIL and the real trajectory when the real path loss exponent η is suddenly changed. (a) Estimated positions and real trajectory. (b) Localization error.

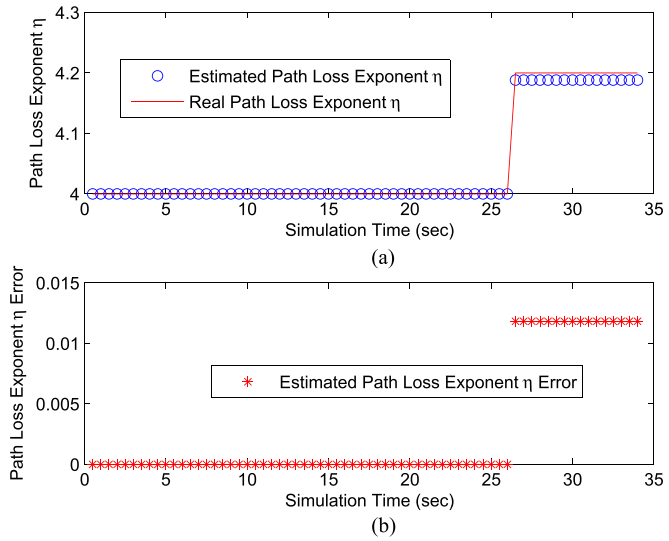

Fig. 9. Comparison of estimated path loss exponent η by CRIL when the real path loss exponent η is suddenly changed. (a) Path loss exponent h. (b) Estimated path loss exponent h error.

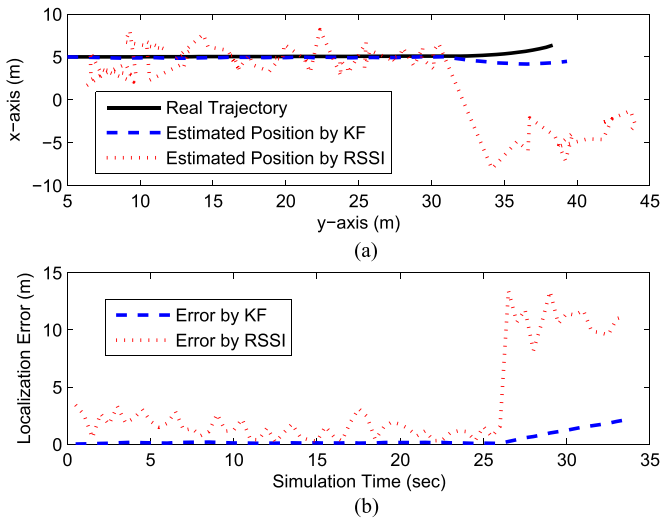

Fig. 11. Comparison of estimated positions by KF [20], RSSI [13] and the real trajectory when the real path loss exponent η is suddenly changed. (a) Estimated positions and real trajecotry. (b) Localization error.

2) Path Loss Exponent η is Suddenly Changed: In this simulation, the value of the path loss exponent η jumps from 4.0 to 4.2 at about $t = 26$ s. This may happen when the mobile object enters one room from another [27]. From Fig. 9, we can find that the estimation error of the path loss exponent η is also very small as that in Figs. 3 and 5, and most of the errors are less than 0.015. We can easily see that the estimated path loss exponent η can track the suddenly changed real path loss exponent η very fast. It is important to notice that the estimation error after $t =$ 26 s is not much different, compared with that before $t = 26$ s. The small error of η caused by the noise and measurement error will not influence the performance of the proposed system too much. Fig. 10 shows that the performance of the proposed CRIL system is very good and not affected by the sudden change of the real path loss exponent η.

Particularly, in Fig. 10, because of the successful detection of the sudden jump of the real path loss exponent η, the proposed system can still output estimated positions with a high accuracy. The performance in this scenario is similar to those in the previous simulations where the real path loss exponent η is a constant or slowly changing. There is not much difference in the estimated error before and after the jump of η, which mostly remains below 0.2 m. This means the performance of the proposed CRIL system is smooth and stable when the parameters are changed suddenly. This is desirable in real-world applications, where a localization system should be adaptive to these changes and update its own parameters effectively. We notice in Fig. 11 that both the RSSI system's and the KF system's localization errors are several meters. Thus, the RSSI [13] and

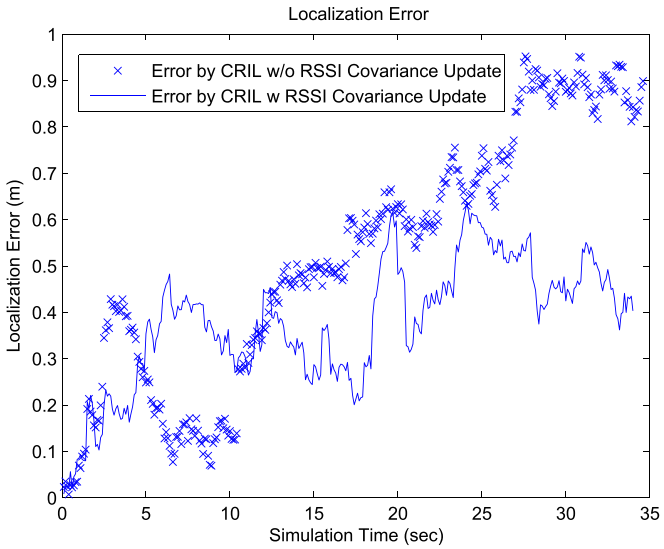

Fig. 12. Comparison of localization errors by CRIL with RSSI covariance update and CRIL without RSSI covariance update when the covariance of RSSI values changes.

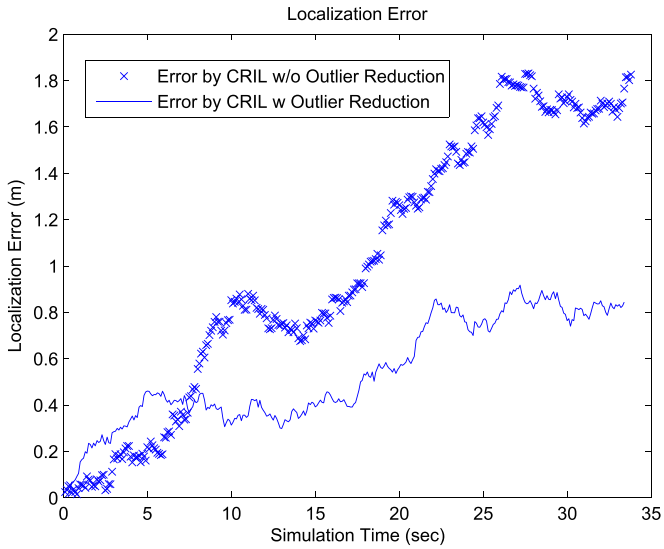

Fig. 13. Comparison of localization errors by CRIL with outlier reduction and CRIL without outlier reduction when the outliers are randomly added into the RSSI values.

KF [20] systems cannot give good localization results because of the sudden changing of the path loss exponent.

D. Results Under Dynamic RSSI Environments

In the previous experiments, the RSSI values is following a fixed Gaussian distribution, and there are no strong outliers in the values. However, based on previous research [13], [27], these are not true in practical environments. In what follows, we discuss and investigate three situations: first, the covariance of RSSI values changes; second, outliers are randomly added into the RSSI values; third, both of the covariance changes and outliers are added into the RSSI values. We show that our CRIL with robust scheme can achieve accurate localization in these situations.

1) Covariance of RSSI Values Changes: In this simulation, the σ of the RSSI values changes from 2 to 4 dBm. In Fig. 12, the estimation errors in the case of CRIL without RSSI covariance update is much bigger than the results in the previous simulations. In contrast, the estimation errors in the case of CRIL with RSSI covariance can give small errors, although they are a little bigger than the results in the fixed RSSI covariance case.

2) Outliers Randomly are Added Into the RSSI Values: In this simulation, the outliers of 15 dBm are randomly added into the RSSI values with the probability of 0.2. In Fig. 13, these outliers lead to big localization errors in the case of CRIL without an outlier reduction. However, the localization errors in the case of CRIL with outlier reduction demonstrate its effect, which give us much better performance.

3) Both of the Covariance Variance and Outliers are Added: In this simulation, both the covariance changes and outliers like those in 1) and 2) are added into the RSSI measurement values. In Fig. 14, the localization errors in the case of CRIL with both the RSSI covariance update and outlier reduction are much smaller than those in the case of CRIL without both RSSI covariance update or outlier reduction. This figure demonstrates that the proposed CRIL scheme can well deal with the uncertainty in RSSI values.

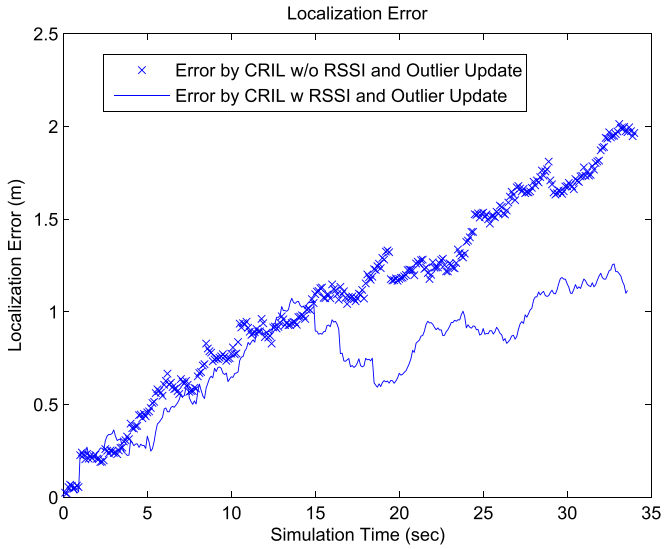

Fig. 14. Comparison of estimated position errors by CRIL with the RSSI covariance update and outlier reduction and CRIL without the RSSI covariance update or outlier reduction when both the covariance changes and outliers are present.

VI. Experiment Results

We conduct experiments on a mobile device (iPhone 5S) to evaluate the performance of our proposed CRIL, which has a tri-gyro and a tri-accelerometer. The IMU data is obtained through the App "Sensor Monitor", and the sampling rate is 120 Hz. The four Wi-Fi anchors are Linksys WRT54GL routers with OpenWrt system. The experiments are done in our lab of 15 m by 10 m. The Wi-Fi anchors are located at the four corners of

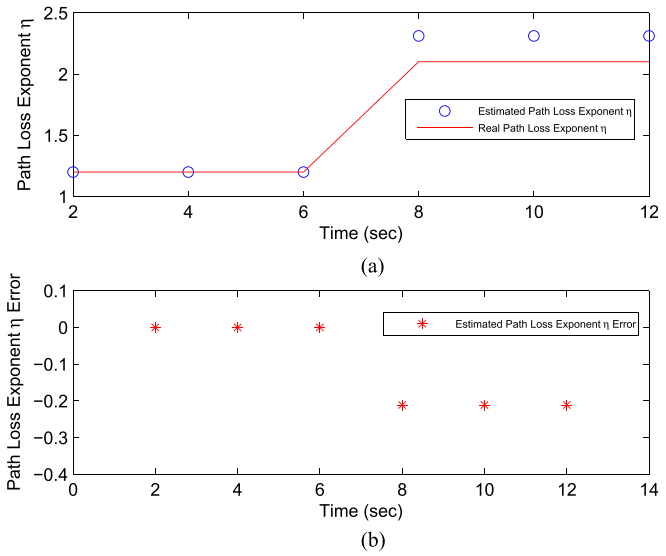

Fig. 15. Comparison of the estimated path loss exponent η by CRIL when the real path loss exponent η is suddenly changed. (a) Path loss exponent h. (b) Extimated path loss exponent h error.

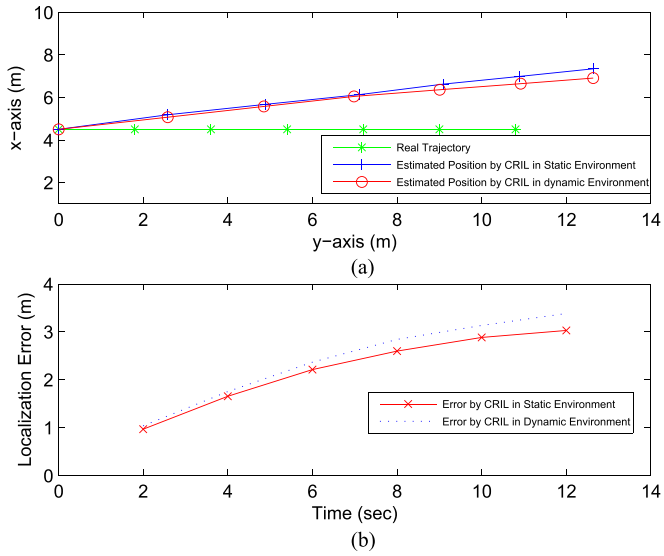

Fig. 16. Comparison of the estimated positions by CRIL in the static environment and in the dynamic environment, with the real trajectory when the real path loss exponent η is suddenly changed. (a) Estimated positions and real trajectory. b) Localization error.

the room and they all cover the whole room. A basic fingerprint system based on k-closest neighbors method [9] is implemented as a comparison of our proposed CRIL system.

In the first experiment, we test our CRIL system with the path loss exponent η jumping from 1.2 to 2.1 at $t = 7$ s. We make it happen by creating many blocks in the room [27]. From Fig. 15, we can find that the estimation error of the path loss exponent η is very small like those in the simulations, and most of the errors are less than 0.25. We can easily see that the estimated path loss exponent η can track the changed real path loss exponent η very fast. The error of η caused by the noise and measurement error will not influence the performance of the proposed system too much.

Besides, Fig. 16 shows that the localization performance of the proposed CRIL system is very good and not affected by the sudden change of the real path loss exponent η. In particular, because of the successful detection of the sudden change in the real path loss exponent η, the proposed CRIL system can still output estimated positions with a high accuracy. There is not much difference in the estimated error with and without the jump of η, which mostly remains below 3 m. This shows that the performance of the proposed CRIL system is good and stable.

In the second experiment, we implement the fingerprint system when the value of the path loss exponent η is 1.2. The same as above, one test is carried out when the environment does not change, and the other is performed when we change the path loss exponent η from 1.2 to 2.1. Besides, each point's RSSI fingerprint is an average of five measurements. We notice in Fig. 17 that in static environment, the average error is 2.4 m, and in the changed environment, the average error is 5.1 m. Obviously, although in the static environment the fingerprint system has a comparable performance with our CRIL system, in the dynamic environment, our CRIL system can maintain good performance and outperform the fingerprint system.

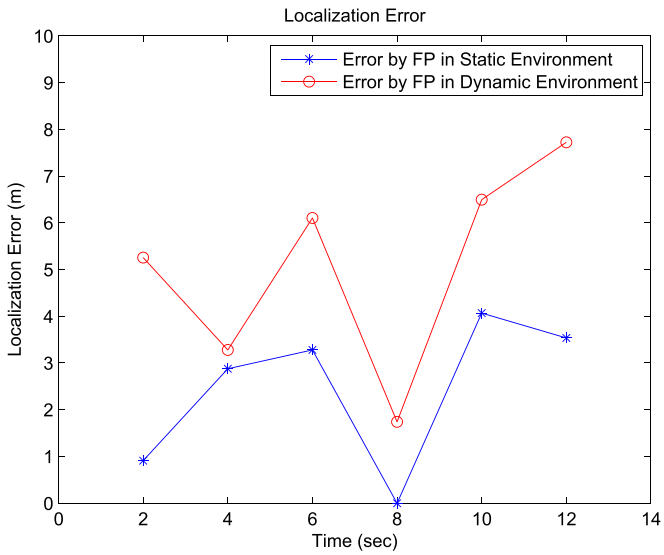

Fig. 17. Comparison of the localization errors by the fingerprint system in the static environment and in the dynamic environment.

VII. Conclusion

Involved in many emerging applications, indoor localization systems have attracted intense research interests recently. This paper has proposed an efficient, adaptive, and robust indoor localization system: CRIL. Generally, the calibration of the channel model in the previous methods is complex, not real time, and time consuming. The proposed CRIL system utilizes the fused results from both the RSSI and INS systems through a newly designed Kalman filter to estimate the object's location while calibrating the channel model in real time. Extensive simulation and experiment studies demonstrate that the proposed system can accurately localize mobile objects. Compared with the previous methods which may not converge and whose localization

errors are several meters or even tens of meters, simulations show that CRIL has much better performance in dynamic environments with localization errors up to 1 m. In particular, CRIL is able to detect the changes in the environment and adapt to dynamic environments quickly and effectively. Moreover, with the outlier reduction and RSSI covariance update, CRIL can still give a good performance when there are more uncertainties in the RSSI values. Finally, through experiments, we prove that our CRIL system works well in practice.

REFERENCES

[1] "Junaio 2.0 first indoor social augmented reality app at sxsw with developers API," [Online]. Available: http://arabcrunch.com/2010/03/junaio-2–0-first-indoor-social-augmented-reality-app-at-sxsw-with-developers-api.html, Mar. 10, 2010.

[2] S. Hemachandra, T. Kollar, N. Roy, and S. Teller, "Following and interpreting narrated guided tours," in *Proc. IEEE Int. Conf. Robot. Autom.*, Shanghai, China, May2011, pp. 2574–2579.

[3] F. Evennou and F. Marx, "Advanced integration of wifi and inertial navigation systems for indoor mobile positioning," *Eurasip J. Appl. Signal Process.*, vol. 2006, pp. 164–164, 2006.

[4] O. Woodman and R. Harle, "Pedestrian localisation for indoor environments," in *Proc. 10th Int. Conf. Ubiquitous Comput.*, Sep. 2008, pp. 114–123.

[5] S. M. George *et al.*, "Distressnet: A wireless ad hoc and sensor network architecture for situation management in disaster response," *IEEE Commun. Mag.*, vol. 48, no. 3, pp. 128–136, Mar. 2010.

[6] L. Taponecco, A. D'Amico, and U. Mengali, "Joint TOA and AOA estimation for UWB localization applications," *IEEE Trans. Wireless Commun.*, vol. 10, no. 7, pp. 2207–2217, Jul. 2011.

[7] C. Zhang, M. Kuhn, B. Merkl, A. Fathy, and M. Mahfouz, "Accurate UWB indoor localization system utilizing time difference of arrival approach," in *Proc. IEEE Radio Wireless Symp.*, San Diego, CA, USA, Oct. 2006, pp. 515–518.

[8] H. Liu, H. Darabi, P. Banerjee, and J. Liu, "Survey of wireless indoor positioning techniques and systems," *IEEE Trans. Syst., Man, Cybern., Part C, Appl. Rev.*, vol. 37, no. 6, pp. 1067–1080, Nov. 2007.

[9] J. Yin, Q. Yang, and L. Ni, "Learning adaptive temporal radio maps for signal-strength-based location estimation," *IEEE Trans. Mobile Comput.*, vol. 7, no. 7, pp. 869–883, Jul. 2008.

[10] J. Wang and D. Katabi, "Dude, where's my card?: RFID positioning that works with multipath and non-line of sight," in *Proc. ACM SIGCOMM*, Hong Kong, China, Aug. 2013, pp. 51–62.

[11] X. Li, "RSS-based location estimation with unknown pathloss model," *IEEE Trans. Wireless Commun.*, vol. 5, no. 12, pp. 3626–3633, Dec. 2006.

[12] T. Sarkar, Z. Ji, K. Kim, A. Medouri, and M. Salazar-Palma, "A survey of various propagation models for mobile communication," *IEEE Antennas Propag. Mag.*, vol. 45, no. 3, pp. 51–82, Jun. 2003.

[13] P. Tarrío, A. M. Bernardos, and J. R. Casar, "Weighted least squares techniques for improved received signal strength based localization," *Sensors*, vol. 11, no. 9, pp. 8569–8592, 2011.

[14] B.-C. Liu, K.-H. Lin, and J.-C. Wu, "Analysis of hyperbolic and circular positioning algorithms using stationary signal-strength-difference measurements in wireless communications," *IEEE Trans. Veh. Technol.*, vol. 55, no. 2, pp. 499–509, Mar. 2006.

[15] P. Barsocchi, S. Lenzi, S. Chessa, and G. Giunta, "A novel approach to indoor RSSI localization by automatic calibration of the wireless propagation model," in *Proc. IEEE 69th Veh. Technol. Conf.*, Barcelona, Spain, Apr. 2009, pp. 1–9.

[16] A. M. Bernardos, J. R. Casar, and P. Tarrío, "Real time calibration for RSS indoor positioning systems," in *Proc. Int. Conf. Indoor Positioning Indoor Navigat.*, Sep. 2010, pp. 1–7.

[17] O. J. Woodman, "An introduction to inertial navigation," Comput. Lab., Univ. Cambridge, Cambridge, U.K., Tech. Rep. UCAMCL-TR-696, 2007.

[18] P. Coronel, S. Furrer, W. Schott, and B. Weiss, "Indoor location tracking using inertial navigation sensors and radio beacons," in *Proc. Internet Things*, 2008, pp. 325–340.

[19] L. Fairfax and F. Fresconi, "Loosely-coupled GPS/INS state estimation in precision projectiles," in *Proc. IEEE/ION Position Location Navigat. Symp.*, Myrtle Beach, SC, USA, Apr. 2012, pp. 620–624.

[20] L. Zwirello, X. Li, T. Zwick, C. Ascher, S. Werling, and G. F. Trommer, "Sensor data fusion in UWB-supported inertial navigation systems for indoor navigation," in *Proc. IEEE Int. Conf. Robot. Autom.*, May 2013, pp. 3154–3159.

[21] J. D. Hol, F. Dijkstra, H. J. Luinge, and P. J. Slycke, "Tightly coupled UWB/IMU pose estimation system and method," US Patent 8 203 487, Jun. 2012.

[22] P. Tarrio, J. Besada, and J. Casar, "Fusion of RSS and inertial measurements for calibration-free indoor pedestrian tracking," in *Proc. 16th Int. Conf. Inf. Fusion.*, Cairns, QLD, Australia, Jul. 2013, pp. 1458–1464.

[23] K. Wu, J. Xiao, Y. Yi, D. Chen, X. Luo, and L. M. Ni, "CSI-based indoor localization," *IEEE Trans. Parallel Distrib. Syst.*, vol. 24, no. 7, pp. 1300–1309, Jul. 2013.

[24] T. Rappaport, *Wireless Communications: Principles and Practice*, 2nd ed. Upper Saddle River, NJ, USA: Prentice-Hall, 2001.

[25] V. Renaudin, B. Merminod, and M. Kasser, "Optimal data fusion for pedestrian navigation based on UWB and MEMS," in *Proc. IEEE/ION Position, Location Navigat. Symp.*, Monterey, CA, USA, May 2008, pp. 341–349.

[26] E. P. Herrera, R. Quirós, and H. Kaufmann, "Analysis of a kalman approach for a pedestrian positioning system in indoor environments," in *Proc. Euro-Par Parallel Process.*, 2007, pp. 931–940.

[27] C. C. Pu, S. Y. Lim, and P. C. Ooi, "Measurement arrangement for the estimation of path loss exponent in wireless sensor network," in *Proc. 7th Int. Conf. Comput. Convergence Technol.*, Seoul, Korea, Dec. 2012, pp. 807–812.

[28] R. G. Stirling, "Development of a pedestrian navigation system using shoe-mounted sensors," , M.S. thesis, Dept. Mech. Eng., Univ. Alberta, Edmonton, AB, Canada, 2003.

[29] A. R. Jimenez, F. Seco, C. Prieto, J. Guevara, "A comparison of pedestrian dead-reckoning algorithms using a low-cost MEMS IMU," in *Proc. IEEE Int. Symp. Intell. Signal Process.*, Budapest, Hungary, Aug. 2009, pp. 37–42.

[30] S. O. Madgwick, A. J. Harrison, and R. Vaidyanathan, "Estimation of IMU and MARG orientation using a gradient descent algorithm," in *Proc. IEEE Int. Conf. Rehabil. Robot.*, Zurich, Switzerland, Jun. 2011, pp. 1–7.

[31] J. Li and D. Xiu, "A generalized polynomial chaos based ensemble kalman filter with high accuracy," *J. Comput. Phys.*, vol. 228, no. 15, pp. 5454–5469, 2009.

[32] S. M. Kay, *Fundamentals of Statistical Signal Processing, Volume III: Practical Algorithm Development*, vol. 3. Upper Saddle River, NJ, USA: Pearson, 2013.

[33] K. Kurashiki, T. Fukao, K. Ishiyama, T. Kamiya, and N. Murakami, "Orchard traveling UGV using particle filter based localization and inverse optimal control," in *Proc. IEEE/SICE Int. Symp. Syst. Integr.*, Shendai, Japan, Dec. 2010, pp. 31–36.

[34] Y. Kaneda, Y. Irizuki, and M. Yamakita, "Design method of robust kalman filter via l_1 regression and its application for vehicle control with outliers," in *Proc. 38th Annu. Conf. IEEE Ind. Electron. Soc.*, Oct. 2012, pp. 2222–2227.

[35] J.-A. Ting, E. Theodorou, and S. Schaal, "A kalman filter for robust outlier detection," in *Proc. IEEE/RSJ Int. Conf. Intell. Robot. Syst.*, San Diego, CA, USA, 2007, pp. 1514–1519.

[36] S. Sarkka and A. Nummenmaa, "Recursive noise adaptive kalman filtering by variational Bayesian approximations," *IEEE Trans. Autom. Control*, vol. 54, no. 3, pp. 596–600, Mar. 2009.

[37] G. Agamennoni, J. I. Nieto, and E. M. Nebot, "An outlier-robust kalman filter," in *Proc. IEEE Int. Conf. Robot. Autom.*, Shanghai, China, 2011, pp. 1551–1558.

[38] J. Mattingley and S. Boyd, "Real-time convex optimization in signal processing," *IEEE Signal Process. Mag.*, vol. 27, no. 3, pp. 50–61, May 2010.

[39] R. Tibshirani, "Regression shrinkage and selection via the lasso," *J. Roy. Stat. Soc., Series B (Methodological)*, vol. 58, pp. 267–288, 1996.

[40] R. K. Mehra, "Approaches to adaptive filtering," *IEEE Trans. Autom. Control*, vol. AC-17, no. 5, pp. 693–698, Oct. 1972.

Authors' photographs and biographies not available at the time of publication.